Reorganization of Functional Connectivity of the Language Network in Patients with Brain Gliomas

C. Briganti
C. Sestieri
P.A. Mattei
R. Esposito
R.J. Galzio
A. Tartaro
G.L. Romani
M. Caulo

BACKGROUND AND PURPOSE: fcMRI measures spontaneous and synchronous fluctuations of BOLD signal between spatially remote brain regions. The present study investigated potential LN fcMRI modifications induced by left hemisphere brain gliomas.

MATERIALS AND METHODS: We retrospectively evaluated fcMRI in 39 right-handed patients with a left hemisphere brain glioma and 13 healthy controls. Patients and controls performed a verb-generation task to identify individual BOLD activity in the left IFG (Broca area); the active region was used as seed to create whole-brain background connectivity maps and to identify the LN (including bilateral regions of the IFG, STS, and TPJ) following regression of task-evoked activity. We assessed differences between patients and controls in the pattern of functional connectivity of the LN, as well as potential effects of tumor position, histopathology, and volume.

RESULTS: Global fcMRI of the LN was significantly reduced in patients with tumor compared with controls. Specifically, fcMRI was significantly reduced within seed regions of the affected hemisphere (left intrahemispheric fcMRI) and between the TPJ of the 2 hemispheres. In patients, the left TPJ node showed the greatest decrease of functional connectivity within the LN.

CONCLUSIONS: The presence of a brain tumor in the left hemisphere significantly reduced the degree of fcMRI between language-related brain regions. The pattern of fcMRI was influenced by tumor position but was not restricted to the area immediately surrounding the tumor because the connectivity between remote and contralateral areas was also affected.

ABBREVIATIONS: BOLD = blood oxygen level–dependent; CS = centrum semiovale; FC = functional connectivity; fcMRI = functional connectivity MRI; IFG = inferior frontal gyrus; LN = language network; STS = superior temporal sulcus; TPJ = temporoparietal junction; V1 = visual area; WHO = World Health Organization

S ince Paul Broca's early clinical observations, the classic theory of cortical organization of language functions has entailed a neural loop involving cortical regions located around the left lateral sulcus, in which Broca and Wernicke areas play leading roles in language production and comprehension, respectively.[1,2] However, this pattern may be modified in patients with brain tumors due to a reorganization of the LN involving both proximal and distal regions relative to the lesion.[3-5]

According to a more recently distributed dynamic model, several widespread functionally connected brain areas compensate for lesions in LN components.[6,7] Thus, the effect of brain lesions may be better evaluated over the entire network rather than on the basis of the activity of isolated regions.

Communicating cortical networks and their dynamics were recently investigated by evaluating the pattern of FC,[8,9] the analysis of spatially distributed and temporally correlated signals in the brain. Resting-state fcMRI is one method used to explore the FC of the LN.[10,11] It measures the temporal correlations in low-frequency (<0.1 Hz) spontaneous fluctuations of BOLD signal between brain regions, without using behavioral tasks.[12,13]

fcMRI has also been used as a useful biomarker of numerous brain disorders; thus, diseases that produce a loss of association fibers and/or changes in synaptic efficiency are thought to alter the communication between neuronal networks. For example, a change in fcMRI of the default mode network may serve as a diagnostic biomarker for onset, progression, and severity of Alzheimer disease[14,15] and schizophrenia.[16] A recent study by Pravatà et al,[17] conducted in a group of patients with intractable epilepsy, found an overall reduction and reorganization of the connectivity pattern within the LN compared with controls, especially in the left hemisphere.

He et al[18] recently investigated modification of fcMRI in patients with stroke with spatial neglect. They found that lesions affecting the ventral attention network[19] caused a disruption of FC between structurally intact regions of the dorsal attention network. Notably, recovery from neglect symptoms was associated with recovery of a normal fcMRI pattern across the dorsal attention network.[18]

In contrast, to our knowledge, modification of FC induced by brain tumors was only observed by using magnetoencephalography. Patients with left hemisphere tumors showed an overall significant reduction of FC compared with healthy controls. This loss was not confined to regions surrounding the tumor but also involved remote areas of the contralesional hemisphere.[20-22]

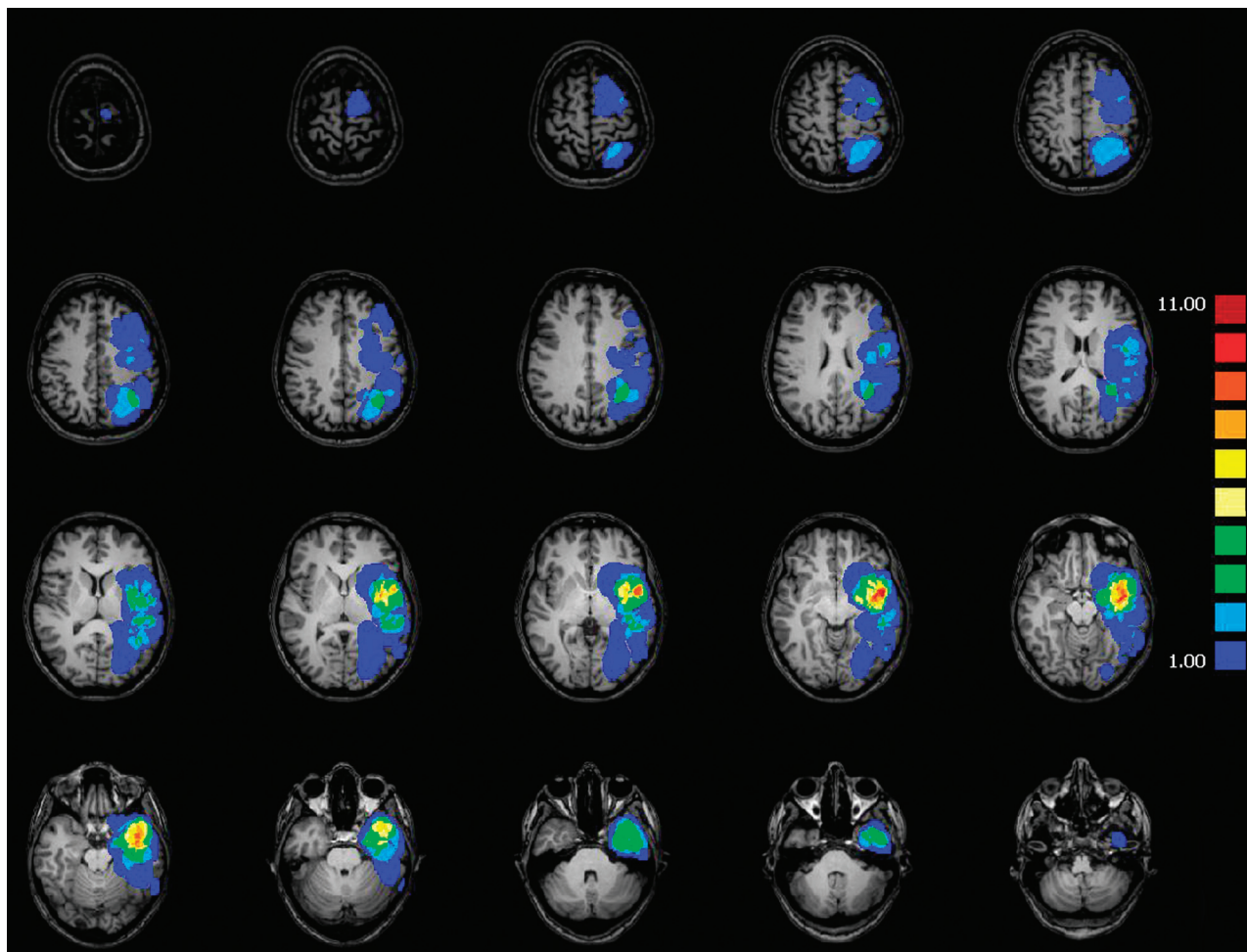In the present study, we measured FC of the LN by using

Fig 1. Degree of left hemisphere glioma overlap across all 39 patients.

fcMRI in patients with left hemisphere brain gliomas and in control subjects to evaluate the impact of left hemisphere tumors. We also evaluated whether the pattern of FC was related to tumor position, histopathology, and volume.

Materials and Methods

Patients and Controls

We retrospectively evaluated 39 patients (21 men and 18 women; age range, 20–70 years; mean age, 51.1 ± 14.0 years) with a histopathologically confirmed surgically naive brain glioma of the left hemisphere. Patients underwent BOLD fMRI to assess language functions for presurgical planning. Inclusion criteria were age >18 years (no upper limit), single left frontal and/or temporoparietal brain glioma, and absence of aphasia. The presence of hydrocephalus and deviations of the midline were exclusion criteria.

A control group of 13 healthy volunteers (7 men and 6 women; age range, 25–64 years; mean age, 40.6 ± 10.9 years) presenting with normal neurologic examination findings underwent the same fMRI protocol.

All subjects had normal hearing and vision and were strongly right-handed as determined by the Edinburgh Handedness Inventory test with a laterality index of >80.[23] Participants gave written informed consent. This study was approved by our local ethics committee.

Lesion Mapping

Among the patients, 12/39 (31%) had frontal; 6/39 (15%), parietal; and 15/39 (38%), temporal lobe tumors, whereas 6/39 (15%) involved temporoparietal sites. Tumors were classified into anterior gliomas ($n = 24/39$, 62%) and posterior gliomas ($n = 15/39$, 38%), according to position with respect to midpoint coordinates in the anteroposterior axis, calculated with averaged coordinates of Broca and Wernicke ROIs ($y = -14$).

Gliomas were divided in 2 subgroups based on the recent WHO classification[24]: 18/39 patients (46%) had low-grade glioma (WHO II), whereas 21/39 (54%) had high-grade glioma (WHO III-IV).

Each tumor was manually segmented by an expert neuroradiologist (M.C.) on the MR images, contouring tumor hypointensity on T1-weighted images under the guidance of T2-weighted images. Corresponding volumes were calculated in cubic millimeters. Tumor volumes ranged from 587 to 79,422 mm^3 (mean, 24,776 ± 20,643 mm^3) (Fig 1).

fMRI Task and Imaging Acquisition

Subjects silently performed an orthographically cued block-designed lexical retrieval verb-generation task, with four 30-second task periods alternated with five 20-second rest periods. During task periods, each noun was presented for 1 second in black letters on a gray background at the center of the screen, followed by a 2-second black fixa-

tion spot during which subjects were instructed to think of pronouncing ≥1 associated verb. During rest periods, subjects relaxed while fixating on a central cross. All participants were asked to silently perform the tasks to avoid head movement. Before scanning, subjects executed a brief overt version of the task to ensure correct performance. As an additional control for correct task execution, at the end of the scan session, participants were asked to retrieve at least 5 words they read during the verb-generation task.

Visual stimuli were presented by using E-Prime, Version 1.1 (Psychology Software Tools, Pittsburgh, Pennsylvania) via an LCD projector and viewed through a mirror placed above the subject's head.

MR imaging data were acquired on a 1.5T system (Magnetom Vision; Siemens, Erlangen, Germany and Achieva; Philips Healthcare, Best, the Netherlands). BOLD functional images were acquired by means of a T2*-weighted echo-planar free-induction-decay sequence with the following parameters: TR, 2000 ms; TE, 60 ms; matrix size, 64 × 64; FOV, 256 mm; in-plane voxel size, 4 × 4 mm; flip angle, 90°; section thickness, 4 mm; no gap. A total of 115 functional volumes were acquired. A high-resolution structural volume was obtained at the end of the session via a 3D gradient-echo T1-weighted sequence with the following parameters: sagittal; TR, 9.7 ms; TE, 4 ms; matrix size, 256 × 256; FOV, 256 mm; in-plane voxel size, 1 × 1 mm; flip angle, 12°; 1-mm section thickness.

fMRI Analysis

Brain Voyager QX Version 1.9 (Brain Innovation, Maastricht, the Netherlands) and custom Matlab scripts (MathWorks, Natick, Massachusetts) were used for data analysis. Preprocessing of functional time series included section time and head-motion correction, linear detrending to remove slow signal drifts, coregistration with anatomic images, and transformation into Talairach anatomic space.[25] None of the extreme cerebral points used for spatial normalization were located within the tumor. An expert neuroradiologist (C.B.) verified the overall accuracy of spatial normalization by calculating the distance between the anterior commissure and lateral points of the hemispheres: Hemispheric differences were evaluated by using a paired t test. No spatial smoothing or high-pass filtering was applied. To evaluate the potential confounding effect of motion artifacts, we quantified individual head shifts along the 3 rotation and 3 translation anatomic axes. To correct for multiple comparisons, we used the false discovery rate approach as formulated for fMRI analysis.[26] In this approach, rather than controlling for the overall number of false-positive voxels (which is sometimes a very conservative choice in fMRI), the number of false-positive voxels among the subset of "suprathreshold" (ie, color-coded) voxels is evaluated. Statistical comparison between groups was performed by using 2-tailed Student t tests.

fcMRI Analysis

fMRI statistical activation maps were generated with a hybrid ICA-general linear model method.[27]

Preprocessing steps for fcMRI analysis[18,28] included the following: 1) bandpass filtering between 0.009 and 0.08 Hz, 2) regression of signals from white matter and ventricles and their first derivatives, 3) regression of brain global signal, 4) regression of 3D motion parameters and their first derivatives, and 5) regression of the deterministic task-evoked components by adding a regressor corresponding to the verb-generation task periods.[29] Data obtained from block-designed fMRI studies are considered to be well-suited for the regression of task-evoked activity and for emulating resting-state

Table 1: ROI 1 averaged Talairach coordinates and SDs in controls and patients

ROI 1 (left IFG)	Controls			Patients		
	X	Y	Z	X	Y	Z
Averaged Talairach coordinates	−49	15	4	−49	17	6
SD	1	3	2	3	5	5

Table 2: ROIs 2–6 averaged Talairach coordinates and SDs in controls and patients

ROI	Controls			Patients		
	X	Y	Z	X	Y	Z
2 (right IFG)						
Averaged Talairach coordinates	47	16	5	45	15	7
SD	2	7	3	5	5	5
3 (left STS)						
Averaged Talairach coordinates	−56	−34	3	−56	−32	1
SD	4	10	6	4	11	6
4 (right STS)						
Averaged Talairach coordinates	57	−35	3	56	−31	3
SD	4	8	4	5	6	5
5 (left TPJ)						
Averaged Talairach coordinates	−54	−43	23	−52	−41	23
SD	2	7	6	4	8	9
6 (right TPJ)						
Averaged Talairach coordinates	54	−42	24	56	−38	22
SD	5	6	5	4	6	6

fcMRI.[29] Therefore, fcMRI analysis was performed over the entire residual dataset. General linear model analysis on the residual dataset was performed in the control group to ensure that no residual BOLD task-evoked activity was present in LN regions.

The fcMRI was calculated with a seed-based method. Because task-evoked BOLD response could be regularly detected only in the left IFG, this region was the first ROI to enter a multistep procedure used to identify other regions of the LN. This first ROI corresponded to the region with maximum BOLD response that was closest to a reference Talairach coordinate (left IFG = x, −49; y, +17; z, +5),[6,30] accounting for eventual anatomic derangement secondary to the tumor (Table 1). An expert neuroradiologist (C.B.) verified the correct localization of ROI 1 in the pars opercularis of the IFG (Broca area, 44/45).

Five additional ROIs located within the LN were identified by using ROI 1 as a seed region in an FC analysis that generated individual voxelwise correlation maps. The BOLD signal time course was averaged across all voxels of ROI 1, and Pearson correlation coefficients (r) between the signal time course of ROI 1 and every voxel of the acquired volume (voxelwise correlation maps) were assessed. Five ROIs were selected by using the region with maximum Pearson correlation coefficients (r) closest to the reference Talairach coordinates obtained in previous studies (right IFG = x, 49; y, +17; z, +5; STS = x, ±55; y, −35; z, +3; TPJ = x, ±55; y, −36; z, +24).[6,30] These regions corresponded to the pars opercularis of the right IFG (ROI 2), the left (ROI 3) and right (ROI 4) STS (Broca area 40), and the left (ROI 5) and right (ROI 6) TPJ (Broca area 22) (Table 2). FLAIR and gadolinium-enhanced MR imaging sequences were used to exclude the possibility that a ROI was positioned within the tumor volume. Statistical comparison of the Talairach coordinates between patients and controls in each ROI was performed by using a 2-tailed t test.

As a result, the FC of the LN was assessed by using these 3 bilateral

homologous ROIs (6-mm radius) identified on individual maps. The BOLD signal time course was averaged across all voxels of each ROI, and Pearson correlation coefficients (*r*) between the signal time course of each ROI pair (pair-wise correlation) were calculated.

To rule out the presence of confounding factors that generally affect fcMRI in patients and to assess the specificity of our results, 4 additional control ROIs (6-mm radius) were placed in the right CS (2 ROIs: r_CS1 and r_CS2) and in the primary visual areas (2 ROIs in the right and left hemisphere: r_V1 and l_V1).

Statistical Analysis
For fcMRI analyses, Pearson correlation coefficients (*r*) were converted into *z* scores by using the Fisher r-to-z transformation.[31] Plots and cross-correlation matrices were used to display significant correlations (*P* < .01) between any ROI pair of the LN. Mean values of fcMRI were estimated within ROIs of the 2 hemispheres (intrahemispheric fcMRI), between homologous ROIs of the 2 hemispheres (inter-IFG fcMRI, inter-STS fcMRI, and inter-TPJ fcMRI), and globally (global fcMRI) by calculating their respective correlation coefficients.[32] Group comparisons (patients versus controls, anterior gliomas versus posterior gliomas, high-grade glioma versus low-grade glioma) between fcMRI values were performed by using an independent-samples 2-tailed *t* test. All analyses were repeated by using a subgroup of patients who were age-matched with the control group. Significant correlations between tumor volume and fcMRI values between ROI pairs were assessed by using Pearson *r* coefficients (*P* < .05).

Results

Introductory Analyses
No significant difference between patients and controls was observed in the distances between anterior commissure and lateral points of the brain (*P* > .05), suggesting that tumors did not compromise spatial normalization. Furthermore, no significant group difference was observed in the amount of head shifts, indicating that potential differences of fcMRI between patients and controls do not depend on head movements. The general linear model analysis performed on the residual dataset in the control group did not show residual BOLD task-evoked activity in any region of the LN at a threshold of *P* < .001. Finally, no significant differences were observed in the Talairach coordinates of the 6 ROIs of the LN between groups.

Task-Evoked fMRI
In the control group, ICA-general linear model analysis of BOLD data for the verb-generation task showed statistically significant activations of the main language-related regions (IFG, STS, and TPJ) in both hemispheres (random-effect analysis, *P* < .01, false discovery rate–corrected). In the patient group, the left IFG was the only region significantly activated in each individual.

fcMRI of the LN
The fcMRI was calculated with a seed-based method by using 3 bilateral spheric ROIs corresponding to nodes of the LN (IFG, STS, and TPJ). Plots and cross-correlation matrices representing fcMRI for control and patient groups are shown in Fig 2. Both controls and patients showed significant correlations among all 6 ROIs of the LN (15 links) (Fig 2*A*, *-B*),

though correlations in patients were reduced compared with those in healthy subjects. Group comparison of fcMRI across ROI pairs (2-tailed *t* test) between patients and controls is shown in Fig 2*C*. Yellow lines indicate significant reduction of fcMRI values (*P* < .01) in patients compared with controls. Notably, the most affected node was the left TPJ.

When we compared the averaged values of fcMRI within and between ROIs of the 2 hemispheres, patients showed a statistically significant reduction of connectivity of the left intrahemispheric, inter-TPJ, and global fcMRI (*P* < .05) (Fig 3). In contrast, analysis of fcMRI across the 4 control ROIs (r_CS1 and r_CS2; r_V1 and l_V1) showed no significant difference between patients and controls, suggesting that the observed results did not simply reflect an unspecific general decrease of connectivity in the group of patients. In addition, the analysis performed with the age-matched subgroup of patients yielded results that were comparable with those obtained with the entire group of patients.

Correlations with Clinical and Tumor Characteristics
In patients, no significant difference in the pattern of fcMRI was found between men and women, and no significant correlation was observed between values of fcMRI and age.

We tested whether tumor position, histopathology, and size affected the pattern of FC of the LN. First, we compared the degree of fcMRI across ROI pairs between patients with anterior gliomas and posterior gliomas (2-tailed *t* test). Plots and cross-correlation matrices of the group comparison are shown in Fig 4.

Comparison of the averaged values of fcMRI within and between ROIs of the 2 hemispheres indicated that the left intrahemispheric fcMRI was significantly reduced in posterior gliomas (mean, 5.84 ± 2.18; range, 0.19–9.22) compared with patients with anterior gliomas (mean, 7.86 ± 2.38; range, 2.77–11.43) (*P* < .05, 2-tailed *t* test). Most interesting, only patients with posterior gliomas showed a significant reduction of the left intrahemispheric fcMRI compared with controls (*P* < .001, 2-tailed *t* test). In contrast, no significant difference in fcMRI patterns within and between ROIs of the 2 hemispheres between patients with low-grade glioma and high-grade glioma was found. Similarly, no significant correlation across subjects was observed between tumor volume and any measure of FC.

Discussion
In the present study, we found the following: 1) The presence of left hemisphere tumors significantly reduced the fcMRI of the LN, particularly affecting connectivity of the left TPJ, 2) both intra- and interhemispheric changes of connectivity were detected, and 3) the pattern of connectivity was modulated by tumor position, with a stronger decrease of left intrahemispheric connectivity in posterior compared with anterior tumors, but not by tumor size or histopathology.

It was proposed that many neurologic disorders that produce a derangement of normal architecture of the brain can alter the communication between neuronal networks.[33] According to this view, the analysis of brain FC is ideally suited to investigate the presence and dynamics of communicating cortical networks. Accordingly, the pattern of connectivity has been found to be altered in several neurologic and psychiatric
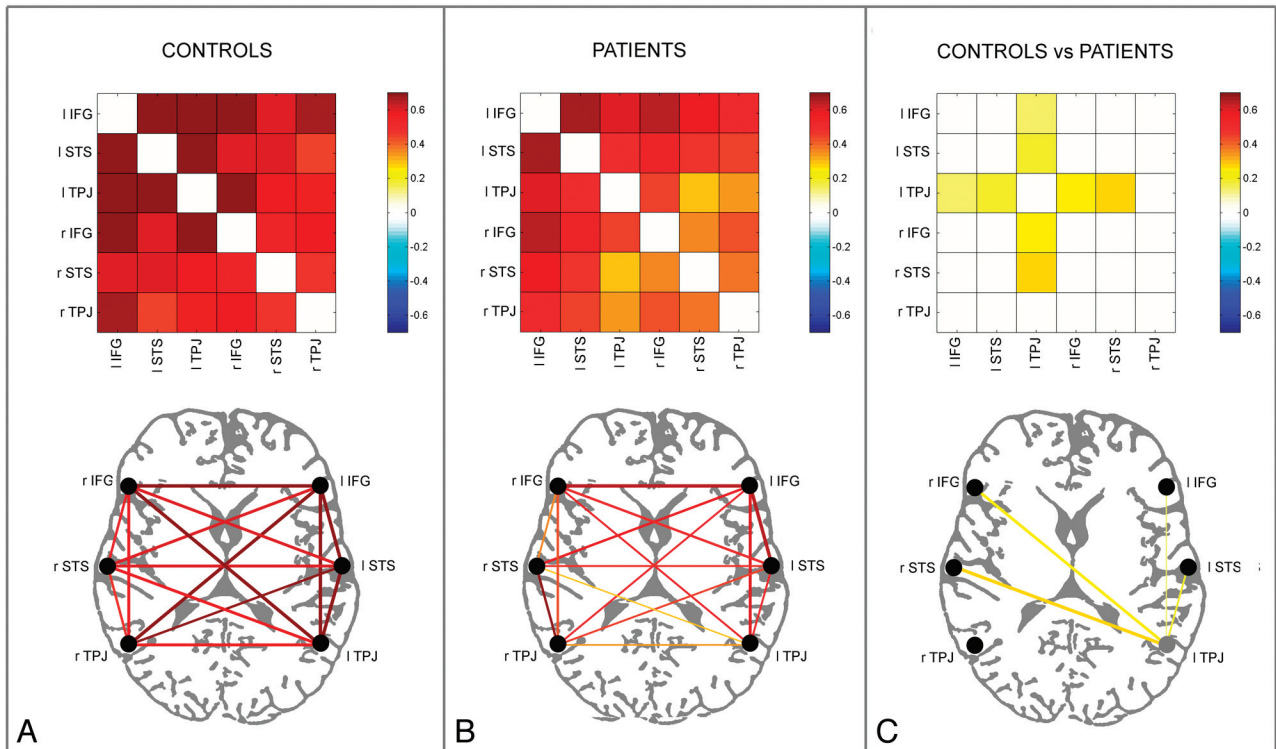
Fig 2. Controls (*n* = 13) (*A*) and patients (*n* = 39) (*B*) color-coded cross-correlation matrices (upper row) and connectivity plots (lower row), representing fcMRI statistically significant links among the 6 ROIs of the LN in the 2 hemispheres through a color-scale, ranging from white (*z* = 0) to dark red (*z* = 0.7) or lines of variable thickness and colors according to the *z* scores, from Pearson coefficient values, respectively. Only statistically significant correlations are shown (*P* < .01). Cross-correlation matrices and connectivity plots representing the statistical comparison between control and patient groups are shown in *C* (independent-samples *t* test, *P* < .01); in the connectivity plot, the lines of variable thickness and yellow tones indicate significantly reduced fcMRI links in patients compared with controls.
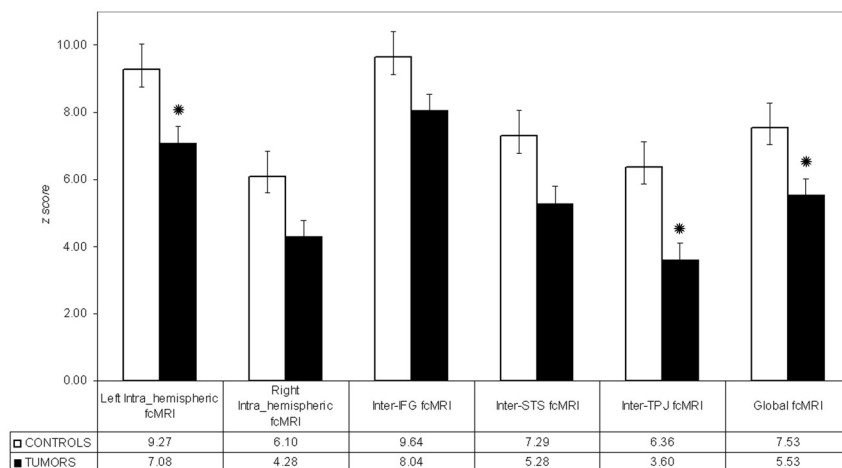

Fig 3. Mean fcMRI values, transformed to *z* scores, within and between the ROIs of the 2 hemispheres in controls and patients. Error bars represent standard error of the mean. Black circles indicate significant differences between groups (*P* < .05, 2-tailed *t* test).

diseases, such as stroke,[18] schizophrenia,[16] neurodegenerative disorders,[34] and epilepsy.[17] Here, by using fcMRI, we confirm initial observations, obtained by using magnetoencephalography, of a reduction of brain connectivity within the LN due to the presence of brain tumors, and we provide further spatial specificity of the results as well as information about the effect of tumor location.

Although the mechanisms by which brain gliomas alter brain functions are not completely understood, it was suggested that tumors infiltrate and compress the cortex and sub-

cortical white matter of language areas, determining a cortical deafferentation and a secondary functional impairment of the disconnected cortex.[35]

When comparing connectivity in patients with tumor against controls, we found that patients showed an overall decrease of connectivity within the LN, which was particularly evident for left hemisphere nodes. Thus, tumors appear to more consistently affect the connectivity within the ipsilesional hemisphere. This "local effect" was bolstered by the observation that tumor location had an impact on the pattern
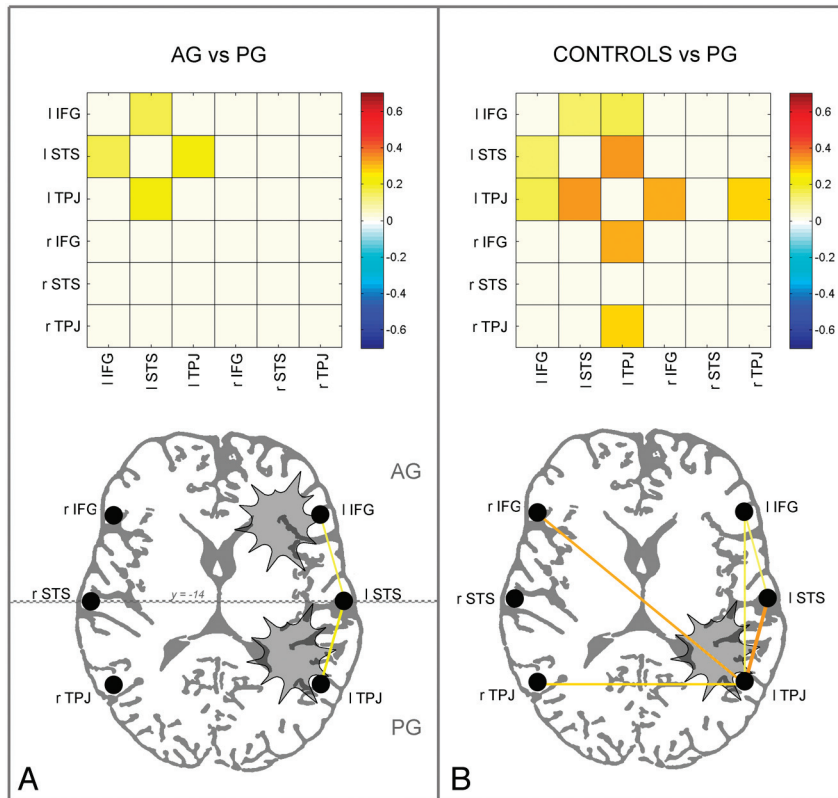
Fig 4. *A*, Cross-correlation matrices and connectivity plots representing the statistical comparison between anterior glioma (*n* = 24) and posterior glioma groups (*n* = 15) (independent-samples *t* test, *P* < .01). In the connectivity plot, the lines of variable thickness and yellow tones indicate significantly reduced fcMRI links in posterior glioma compared with anterior glioma. *B*, Cross-correlation matrices and connectivity plots representing the statistical comparison between controls (*n* = 13) and the posterior glioma group (*n* = 15) (independent-samples *t* test, *P* < .01). In the connectivity plot, the yellow lines of variable thickness and yellow tones indicate significantly reduced fcMRI links in posterior glioma compared with controls; the most affected node was left TPJ. Patients with anterior glioma did not show significant differences in fcMRI compared with controls.

of connectivity so that posterior gliomas had a greater effect on TPJ connectivity. Most interesting, a recent study that investigated theoretic models of FC showed that lesions involving high-centrality nodes (hubs), such as the TPJ, induced larger and more widespread FC pattern effects.[36] Although these results come from different fields of research, overall they underline the crucial role of the TPJ for the integrity of functional networks, while suggesting a particular vulnerability of this cortical area to local and nonlocal disturbances. On a side note, the presence of FC differences between anterior and posterior tumors also suggests that the present results were not caused by unspecific hemodynamic modifications induced by medication or by vasoactive substances and/or neuro-transmitters released by tumors because these factors should produce comparable effects in both subgroups.

In addition, given the widespread properties of cortical networks and the intrinsic nature of connectivity analysis, which assesses the degree of correlation between remote cortical nodes, the presence of lesions also had "distant effects." First, a reduction of connectivity was generally observed between nodes that did not overlap with tumor location, according to the currently available methods for lesion segmentation. Second, changes induced by tumors included an alteration of interhemispheric connectivity, thus affecting the normal communication between hemispheres. The functional significance of distant interhemispheric communication was recently demonstrated by He et al.[18] The authors showed that behavioral performance in neglect patients was associated with in-

terhemispheric connectivity between structurally intact regions of the parietal cortex, which was altered by lesions of another network, due to internetwork dysfunctional interactions. Furthermore, Carter et al[32] recently showed that cortical lesions can modify the spontaneous coherence between close and distant regions belonging to a functional network and even between other related functional networks. Considered together, these results argue against the adoption of a strict localization approach and suggest that the effect of a lesion goes beyond the affected area.

Notably, both tumor size and histopathologic classification did not significantly modulate the pattern of FC observed in this study. Although more research is needed to confirm the present results, we suggest that the lack of sensitivity of fcMRI to these indices may be due to 2 factors: First, low-grade glioma and high-grade glioma are equally slow-growing lesions compared with the time required for brain reorganization; thus, they could produce similar effects on the pattern of connectivity. Also, patients with aphasia, which could be caused by larger tumors, were intentionally excluded from this study, minimizing functional differences across groups.[27]

There are several reasons for using fcMRI for clinical applications. The most obvious is that in general, fcMRI does not necessarily require the execution of any specific language task, allowing the simultaneous assessment of FC within and between multiple cortical systems with only minimal demand on patients.[37] In addition, the assessment of FC is theoretically less influenced by modification of the normal hemodynamic

response compared with standard analysis of task-evoked activity. This is particularly relevant for the present group of patients, in whom the tumor may have altered a normal neurovascular coupling.

Crucially, the analysis of FC, especially in the diseased brain, allows the assessment of the functional integrity of a network as a whole. This is in accordance with a more recent network perspective, which suggests that the effect of brain lesions needs to be evaluated on the entire network, rather than at the level of single regions.[6,7] Finally, resting state FC can also be used for preoperative identification of the eloquent cortex in patients with brain tumors.[38] With magnetoencephalography, it was shown that regions with reduced FC have a negative predictive value for the presence of eloquent cortex during intraoperative electrical stimulation,[39] theoretically allowing safe and complete resection of the area.

Nonetheless, we must consider potential limitations of the present study, mostly related to the comparison between patients and controls. First, tumors may distort the normal brain anatomy, potentially dislocating eloquent cortical regions. To preserve intersubject comparability, we excluded patients with lesions crossing the midline, which particularly compromise spatial normalization. FC was calculated with a seed-based method by using spheric ROIs identified in each individual, to control for modifications of anatomic structures induced by tumors and to eliminate the possibility that a ROI was positioned within the tumor. However, this method does not exclude the presence of microscopic, therefore intrinsically unascertainable with MR imaging, infiltration by the tumor into surrounding brain tissue. Because the pars opercularis of the left IFG was the only region constantly detectable in each subject by using task-evoked BOLD activity, the peak of activity in this region was used as a first seed to obtain individual voxelwise correlation maps, in which all the language-related areas were always detectable. A possible concern is that fcMRI may be altered by the use of connectivity maps to select seed regions, though we think that potential bias of the fcMRI procedure is overcome by the use of the same method in patients and controls.

Second, various sources of artifacts may selectively affect the assessment of connectivity in the group of patients. Increased movement may have a negative effect on the estimate of the BOLD response to task conditions and on the assessment of FC. To rule out this possibility, we compared the amount of head shifts along the 3 rotation and 3 translation axes and found no differences. The presence of group differences related to the general effect of cardiac and respiratory cycles or movements was further excluded by assessing connectivity between additional control ROIs,[40] which did not show a significant group difference.

Third, task performance may vary between individuals and may result in different patterns of connectivity. Although we enrolled only cooperative patients without aphasia and indirectly controlled for correct task execution, our task did not provide a measure of performance. It has been reported that task execution enhances inter-regional connectivity that is already present at rest in the corresponding network,[41] and this finding also applies to language tasks.[11] To minimize performance confounds, fcMRI analysis was performed on the residual dataset obtained by removing the deterministic task-evoked components of the BOLD signal,[29] a procedure that has been proved to work adequately in combination with block designs.[29] The presence of residual task-evoked activity was further excluded by looking at the efficacy of task regression in control subjects. Because no systematic investigation has been conducted concerning the effects of effort on FC, once the task-evoked activity has been removed, it is difficult to make predictions about the direction of potential effects related to effort. Nonetheless, the presence of a stronger reduction of FC in a specific group of patients, in the absence of a concurrent change of connectivity between sensory (visual) regions, is not consistent with the idea that performance/effort had a significant role in the current study.

Finally, we did not investigate potential modifications of the pattern of connectivity among functional networks other than language. However, in the absence of individual task-evoked activity to map other cognitive functions, we preferred to adopt a conservative approach and rely on individual activation data to guide the fcMRI analysis. As a matter of fact, the presence of tumors discouraged us from using standard ROIs derived from the literature because these ROIs may fall inside the tumors, compromising the analysis of connectivity.

Conclusions

This study explored the effect of left hemisphere brain gliomas on LN fcMRI. We showed that compared with controls, patients presented a global reduction of FC within the LN. The presence of a tumor influenced connectivity in the ipsilesional hemisphere correlated with tumor location, and also had distant effects in terms of loss of interhemispheric connectivity.

References

1. Broca P. **Remarques sur le siege de la faculte du langage articule, suivie d'une observation d'aphemie (perte de la parole).** *Bulletin de la Société Anatomie* 1861;6:330–57

2. Binder JR, Frost JA, Hammeke TA, et al. **Human brain language areas identified by functional magnetic resonance imaging.** *J Neurosci* 1997;17:353–62

3. Thiel A, Herholz K, Koyuncu A, et al. **Plasticity of language networks in patients with brain tumors: a positron emission tomography activation study.** *Ann Neurol* 2001;50:620–29

4. Desmurget M, Bonnetblanc F, Duffau H. **Contrasting acute and slow-growing lesions: a new door to brain plasticity.** *Brain* 2007;130:898–914

5. Duffau H. **New concepts in surgery of WHO grade II gliomas: functional brain mapping, connectionism and plasticity: a review.** *J Neurooncol* 2006;79:77–115

6. Vigneau M, Beaucousin V, Hervé PY, et al. **Meta-analyzing left hemisphere language areas: phonology, semantics, and sentence processing.** *Neuroimage* 2006;30:1414–32

7. Xiang HD, Fonteijn HM, Norris DG, et al. **Topographical functional connectivity pattern in the perisylvian language networks.** *Cereb Cortex* 2010;20:549–60

8. Van den Heuvel MP, Hulshoff Pol HE. **Exploring the brain network: a review on resting-state fMRI functional connectivity.** *Eur Neuropsychopharmacol* 2010;20:519–34

9. Pillai JJ. **Insights into adult postlesional language cortical plasticity provided by cerebral blood oxygen level-dependent functional MR imaging.** *AJNR Am J Neuroradiol* 2010;31:990–96

10. Matsumoto R, Nair DR, LaPresto E, et al. **Functional connectivity in the human language system: a cortico-cortical evoked potential study.** *Brain* 2004;127:2316–30

11. Hampson M, Peterson BS, Skudlarski P, et al. **Detection of functional connectivity using temporal correlations in MR images.** *Hum Brain Mapp* 2002;15:247–62

12. Fox MD, Snyder AZ, Vincent JL, et al. **The human brain is intrinsically organized into dynamic, anticorrelated functional networks.** *Proc Natl Acad Sci U S A* 2005;102:9673–78

13. Fransson P. **Spontaneous low-frequency BOLD signal fluctuations: an fMRI investigation of the resting-state default mode of brain function hypothesis.** *Hum Brain Mapp* 2005;26:15–29

14. Greicius MD, Srivastava G, Reiss AL, et al. **Default-mode network activity dis-**

tinguishes Alzheimer's disease from healthy aging: evidence from functional MRI. *Proc Natl Acad Sci U S A* 2004;101:4637–42

15. Buckner RL, Sepulchre J, Talukdar T, et al. **Cortical hubs revealed by intrinsic functional connectivity: mapping, assessment of stability, and relation to Alzheimer's disease.** *J Neurosci* 2009;29:1860–73

16. Whitfield-Gabrieli S, Thermenos HW, Milanovic S, et al. **Hyperactivity and hyperconnectivity of the default network in schizophrenia and in first-degree relatives of persons with schizophrenia.** *Proc Natl Acad Sci U S A* 2009;106:1279–84

17. Pravata E, Sestieri C, Mantini D, et al. **Functional connectivity MR imaging of the language network in patients with drug-resistant epilepsy.** *AJNR Am J Neuroradiol* 2011;32:532–40

18. He BJ, Snyder AZ, Vincent JL, et al. **Breakdown of functional connectivity in frontoparietal networks underlies behavioral deficits in spatial neglect.** *Neuron* 2007;53:905–18

19. Corbetta M, Shulman GL. **Control of goal-directed and stimulus-driven attention in the brain.** *Nat Rev Neurosci* 2002;3:201–15

20. Bartolomei F, Bosma I, Klein M, et al. **How do brain tumors alter functional connectivity? A magnetoencephalography study.** *Ann Neurol* 2006;59:128–38

21. Guggisberg AG, Honma SM, Findlay AM, et al. **Mapping functional connectivity in patients with brain lesions.** *Ann Neurol* 2008;63:193–203

22. Douw L, Baayen H, Bosma I, et al. **Treatment-related changes in functional connectivity in brain tumor patients: a magnetoencephalography study.** *Exp Neurol* 2008;212:285–90

23. Oldfield RC. **The assessment and analysis of handedness: the Edinburgh inventory.** *Neuropsychologia* 1971;9:97–113

24. Louis DN, Ohgaki H, Wiestler OD, et al. **The 2007 WHO classification of tumours of the central nervous system.** *Acta Neuropathol* 2007;114:97–109

25. Talairach J, Tournoux P. *Co-Planar Stereotaxic Atlas of the Human Brain.* New York: Thieme; 1988

26. Genovese CR, Lazar NA, Nichols T. **Thresholding of statistical maps in functional neuroimaging using the false discovery rate.** *Neuroimage* 2002;15:870–78

27. Caulo M, Esposito R, Mantini D, et al. **Comparison of hypothesis- and a novel hybrid data/hypothesis-driven method of functional MR imaging analysis in patients with brain gliomas.** *AJNR Am J Neuroradiol* 2011;32:1056–64

28. Vincent JL, Snyder AZ, Fox MD, et al. **Coherent spontaneous activity identifies a hippocampal-parietal memory network.** *J Neurophysiol* 2006;96:3517–31

29. Fair DA, Schlaggar BL, Cohen AL, et al. **A method for using blocked and event-related fMRI data to study "resting state" functional connectivity.** *Neuroimage* 2007;35:396–405

30. Seghier ML, Lazeyras F, Pegna AJ, et al. **Variability of fMRI activation during a phonological and semantic language task in healthy subjects.** *Hum Brain Mapp* 2004;23:140–55

31. Zar JH. *Biostatistical Analysis.* Upper Saddle River, New Jersey: Prentice-Hall; 1996:768–72

32. Carter AR, Astafiev SV, Lang CE, et al. **Resting interhemispheric functional magnetic resonance imaging connectivity predicts performance after stroke.** *Ann Neurol* 2010;67:365–75

33. Oshino S, Kato A, Wakayama A, et al. **Magnetoencephalographic analysis of cortical oscillatory activity in patients with brain tumors: synthetic aperture magnetometry (SAM) functional imaging of delta band activity.** *Neuroimage* 2007;34:957–64

34. Seeley WW, Crawford RK, Zhou J, et al. **Neurodegenerative diseases target large-scale human brain networks.** *Neuron* 2009;62:42–52

35. Kamada K, Moller M, Saguer M, et al. **A combined study of tumor-related brain lesions using MEG and proton MR spectroscopic imaging.** *J Neurol Sci* 2001;186:13–21

36. Alstott J, Breakspear M, Hagmann P, et al. **Modeling the impact of lesions in the human brain.** *PLoS Comput Biol* 2009;5:1–12

37. Fox MD, Greicius M. **Clinical applications of resting state functional connectivity.** *Front Syst Neurosci* 2010;17:4–19

38. Zhang D, Johnston JM, Fox MD, et al. **Preoperative sensorimotor mapping in brain tumor patients using spontaneous fluctuations in neuronal activity imaged with functional magnetic resonance imaging: initial experience.** *Neurosurgery* 2009;65:226–36

39. Martino J, Honma SM, Findlay AM, et al. **Resting functional connectivity in patients with brain tumors in eloquent areas.** *Ann Neurol* 2011;69:521–32

40. Cordes D, Haughton VM, Arfanakis K, et al. **Mapping functionally related regions of brain with functional connectivity MR imaging.** *AJNR Am J Neuroradiol* 2000;21:1636–44

41. Fox MD, Raichle ME. **Spontaneous fluctuations in brain activity observed with functional magnetic resonance imaging.** *Nat Rev Neurosci* 2007;8:700–11